THE ROYAL SOCIETY

Received 13 June 2002
Accepted 11 September 2002
Published online 19 November 2002

Space and the persistence of male-killing endosymbionts in insect populations

Maria A. C. Groenenboom* **and Paulien Hogeweg**

Theoretical Biology and Bioinformatics, University of Utrecht, Padualaan 8, 3584 CH Utrecht, The Netherlands

Male-killing bacteria are bacteria that are transmitted vertically through the females of their insect hosts. They can distort the sex ratio of their hosts by killing infected male offspring. In nature, male-killing endosymbionts (male killers) often have a 100% efficient vertical transmission, and multiple male-killing bacteria infecting a single population are observed. We use different model formalisms to study these observations. In mean-field models a male killer with perfect transmission drives the host population to extinction, and coexistence between multiple male killers within one population is impossible; however, in spatially explicit models, both phenomena are readily observed. We show how the spatial pattern formation underlies these results. In the case of high transmission efficiencies, waves with a high density of male killers alternate with waves of mainly wild-type hosts. The male killers cause local extinction, but this creates an opportunity for uninfected hosts to re-invade these areas. Spatial pattern formation also creates an opportunity for two male killers to coexist within one population: different strains create spatial regions that are qualitatively different; these areas then serve as different niches, making coexistence possible.

Keywords: male killing; mathematical model; selfish genetic element; *Wolbachia*; sex ratio; polymorphism

1. INTRODUCTION

Maternally inherited symbiotic bacteria are common in insects. One much-studied example is *Wolbachia*, which possibly infects more than 17–22% of all insect species (Jiggins *et al.* 2001*a*). As bacteria in males cannot be transmitted to the next generation, the bacteria often favour the female of their host species. They do this by distorting host reproduction in a variety of ways, including cytoplasmic incompatibility (Hoffmann & Turelli 1997), feminization of genetic males (Rousset *et al.* 1992), parthenogenesis (Stouthamer *et al.* 1993) and male killing (Hurst *et al.* 1992).

Here, we focus on early male killing, in which the infected male is killed early in embryonic development. As bacteria in males are not transmitted, the death of infected male hosts has no direct negative effect on the spread of the bacteria. It could be argued that male killing carries benefits to the hosts, which may then indirectly benefit the bacteria, through reduced competition and cannibalism (Hurst *et al.* 1997). This has been generally accepted as the main advantage (for both the bacteria and the hosts) of male killing.

In the field, vertical transmission efficiencies have been observed to range from 72% to 100%, with most observations being close to perfect (Jiggins *et al.* 1998, 2000; Majerus *et al.* 1998, 2000). Research on a population of the two-spotted ladybird, *Adalia bipunctata*, in Moscow, showed that four strains of male-killing bacteria with different transmission efficiencies can coexist within a single population: two different *Wolbachia* (Hurst *et al.* 1999*b*), a *Spiroplasma* (Hurst *et al.* 1999*a*) and a *Rickettsia* (Werren *et al.* 1994) were found. A study on the Common Acreae butterfly (*Acraea encedon*), in Tanzania, also showed two different strains of *Wolbachia* within a single population (Jiggins *et al.* 2001*b*). However, there is at most one male-killer species present per individual host (Majerus *et al.* 2000).

Previously, a number of mathematical models have been developed to describe a host population with male-killing bacteria in terms of vertical transmission efficiency, and positive and negative effects of infection (Hurst 1991; Hurst *et al.* 1997; Freeland & McCabe 1997; Randerson *et al.* 2000). Using a discrete generation model, Hurst (1991) showed that invasion of a male killer is only possible when both the vertical transmission is imperfect (described by $\alpha < 1$) and there is a positive effect on the fitness of the female host of carrying the infection. In his model, a perfectly transmitted male killer reaches a frequency in the population of 1, and therefore he concludes that the population becomes extinct. Randerson *et al.* (2000) showed in a similar model that two male killers with different transmission efficiencies cannot coexist within a single population: the male killer with the higher transmission rate or the higher positive fitness effect on the host will outcompete the other. In their model, two male killers can only be maintained within a single population if hosts develop resistance genes against the winning 'fitter' male killer. However, evidence for such resistance genes has not yet been obtained.

None of the previous studies can explain the recent observations of the existence of perfectly transmitted male killers or the polymorphism. Moreover, combining the above-cited results, one should infer that evolution always selects for higher transmission rates, and hence, in the long run, extinction is inevitable.

In this study, we show that the discrepancies between the empirical data and the model studies published to date are caused by the use of mean-field models. We show that a perfectly transmitted male killer in a spatial setting can

*Author and address for correspondence: Theoretical Biology and Bioinformatics, University of Utrecht, Padualaan 8, 3584 CH Utrecht, The Netherlands (m.a.c.groenenboom@bio.uu.nl).

invade without driving the population to extinction, and that two male killers with different transmission efficiencies can permanently coexist within a single population.

2. MODEL DESCRIPTION

(a) *Basic details*

We use a spatial model and two mean-field models to describe a system of hosts and male-killing bacteria. More specifically, we use two cellular automata (CA) models and an ordinary differential equation (ODE) model.

All three models are based on the same explicit assumptions. The only differences lie in the assumptions implicit in the different formalisms. In all three models, the bacteria are transmitted via the females, and all infected males die. Transmission of the bacteria is strictly vertical, and its efficiency (α) can be varied from 0 to 100%. There are no explicit differences between infected and uninfected individuals: they all have the same death rate (δ). There is sexual reproduction, and females produce eggs in a 1 : 1 sex ratio. An infected female produces α infected offspring and $(1-\alpha)$ uninfected offspring.

In nature, neonates suffer from strong food competition and often fail to obtain the amount of food necessary for survival (Banks 1955). Since $\alpha/2$ of the offspring of an infected female will not hatch (i.e. the infected male eggs), the hatched individuals suffer less competition, resulting in a higher survival chance for the siblings of dead males. The reduced competition or the cannibalism of dead brothers could, in the most extreme case, fully compensate for the fact that a part of the clutch does not hatch. Note that when $\alpha < 1$ the uninfected siblings also have a higher chance of survival. The fraction of surviving offspring is $(1-\alpha)+\alpha/2$. We denote the increased survival chance by r, where r is 1 (the wild-type fitness) plus the fitness gained from the dead brothers. To describe incomplete fitness compensation we add a parameter, c, which is the fraction of the full compensation:

$$r = 1 + c\frac{\frac{1}{2}\alpha}{(1-\alpha)+\frac{1}{2}\alpha} = 1 + \frac{c\alpha}{2-\alpha}, \quad 0 \leqslant c \leqslant 1. \tag{2.1}$$

In their studies, Hurst (1991) and Randerson *et al.* (2000) used similar formulae.

(b) *The spatial model*

We use a stochastic CA model. Each automaton represents an insect, which can be in an infected or uninfected state. The neighbourhood of each individual consists of the eight adjacent automata.

One time-step in the model represents the approximate time needed for reproduction; during this time each female can produce offspring if there is a male available in her neighbourhood. A clutch of offspring is then put at the same location as the female. After reproduction, the adult insects have a random probability of dying.

In our model, we use the two-spotted ladybird as an example. The two-spotted ladybird can reproduce up to twice a year, so one time-step equals half a year. The probability of dying is set to 40%, which means that 60% of the insects can reproduce again during the next reproductive season.

As the number of available automata is limited, the offspring have to compete for space; this is equivalent to the competition for limiting resources in the biological system. Each empty automaton is occupied by an individual randomly selected from, at most, nine clutches laid in the direct neighbourhood (the given automaton plus its eight adjoining sites). During this random draw, we take into account the fact that the fractions of males and (un)infected females can vary, as can the clutch sizes (see table 1). If there are no clutches in the direct neighbourhood, the space remains empty. After this 'maturation' process, all clutches are removed from the CA.

Each time-step the insects move around randomly. We use one step of Margolus diffusion (Toffoli & Margolus 1987) to avoid conflicts during random motion. We start each simulation with a population of uninfected hosts (in a field of 200×200 automata). Within a small patch (of 5×5 automata) we infect all the females with the male killer. There is no minimum initial number of infected individuals required. We infect a patch of hosts instead of only one host to prevent extinction of the male killer as a result of stochasticity.

For a more detailed description of the spatial model see table 1.

(c) *Mean-field models*

We used two different mean-field approximations of the spatial model described in § 2b.

The first model is deterministic and assumes global interactions. It is formulated as a set of three ODEs for the fraction of space occupied by infected females (F_i), uninfected females (F_u) and (uninfected) males (M), respectively. Sexual reproduction, fitness compensation, vertical transmission and competition are all in accordance with the spatial model. Time is scaled to the maximum growth rate, i.e. the model is non-dimensional. A fraction $(1 - F_i - F_u - M)$ of the space is empty. This is an important difference between our model and previous models, in which the populations always summed to 1. Competition is represented by a product of the reproduction term and the empty space available.

$$\frac{dF_i}{dt} = \frac{1}{2}r\alpha F_i M(1 - F_i - F_u - M) - \delta F_i, \tag{2.2a}$$

$$\frac{dF_u}{dt} = \frac{1}{2}F_u M(1 - F_i - F_u - M) - \delta F_u + \frac{1}{2}r(1-\alpha)F_i M(1 - F_i - F_u - M), \tag{2.2b}$$

$$\frac{dM}{dt} = \frac{1}{2}F_u M(1 - F_i - F_u - M) - \delta M + \frac{1}{2}r(1-\alpha)F_i M(1 - F_i - F_u - M), \tag{2.2c}$$

where δ is the death rate, r is the fitness compensation (as defined by equation (2.1)) and α is the vertical transmission efficiency. As equations (2.2*b*) and (2.2*c*) have precisely the same form, the numbers of (uninfected) males and uninfected females converge. For mathematical analysis we can, therefore, substitute M by F_u and study the following two-dimensional (2D) system:

$$\frac{dF_i}{dt} = \frac{1}{2}r\alpha F_i F_u(1 - F_i - 2F_u) - \delta F_i, \tag{2.3a}$$

Table 1. Description of the CA model consisting of 200 × 200 automata, with next-state probabilities (p) for each automaton. (Each time-step consists of three stages. The program was written in C, using the CASH libraries for CA (http://www-binf.bio.uu.nl/rdb/software.html))

1. Reproduction and death:
for each automaton:
  if automaton is occupied by female host
    if male in one of eight adjacent automata
      → uninfected female produces uninfected clutch
      → infected female produces infected clutch
  → automaton becomes empty with probability δ (note that clutches remain in place if host is removed)

2. Competition and hatching:
for each automaton:
  if automaton is empty
    list the nine adjacent automata in random order
    if first adjacent automaton in list contains
      uninfected clutch
        → p(uninfected female) = 0.5
        → p(uninfected male) = 0.5
      infected clutch
        → p(uninfected female) = $0.5r(1-\alpha)$
        → p(uninfected male) = $0.5r(1-\alpha)$
        → p(infected female) = $0.5r\alpha$
        → p(empty) = $0.5r\alpha$
    if automaton is still empty, repeat procedure for next adjacent automaton in list

3. Migration:
for each automaton:
  → move by means of one step of Margolis diffusion; in this way each host migrates to a random adjacent automata

Notes: males are promiscuous; a clutch can produce more than one adult (maximally nine), depending on local competition; the migration of males and females is the same.

$$\frac{dF_u}{dt} = \frac{1}{2}F_u^2(1 - F_i - 2F_u) - \delta F_u + \frac{1}{2}r(1-\alpha)F_iF_u(1 - F_i - 2F_u). \quad (2.3b)$$

The second mean-field model preserves the localness of interactions and the stochasticity of the spatial model. It is identical to the spatial CA model, but at each time-step each position is switched with a random position in the field, i.e. all entities (states) are randomly distributed over the field. By formulating the model in this way, we can be sure that any difference in its behaviour relative to the spatial model must be entirely due to self-organized spatial patterns.

3. ANALYSIS OF THE ODE MODEL

We start by analysing the ODE model, as this model most closely corresponds to previous model approaches. The reduced model allows for 2D phase plane analysis. Bifurcation analysis shows that in this model there are four regions with qualitatively different behaviour.

(a) *Bifurcation diagram*

In figure 1*a* we have plotted the bifurcation diagram for the transmission efficiency, α, and the fitness compensation, c. Three regions are separated by two bifurcation lines in the (α,c) plane. The line on the left represents two co-occurring transcritical bifurcations. The position of the line is independent of δ and is given by

$$c = 1 - \frac{3}{\alpha} + \frac{2}{\alpha^2}. \quad (3.1)$$

The line on the right is a line of fold bifurcations. The position of this line depends on δ and is given by

$$c = \frac{\alpha(\alpha - 1 - 4\delta) + 8\delta - 2\sqrt{2\alpha^2\delta - 2\alpha\delta + 4\alpha^2\delta^2 - 16\alpha\delta^2 + 16\delta^2}(\alpha - 2)}{\alpha(\alpha^2 - \alpha)}. \quad (3.2)$$

It can be easily shown that the line of fold bifurcations can be shifted from vertical (at $\lim\delta \downarrow 0$), to lying on top of the line of transcritical bifurcations (at $\lim\delta \uparrow 1/16$). For the derivation of the bifurcation lines (equations (3.1) and (3.2)) see Appendices A–C.

When $\delta = 1/16$, another fold bifurcation occurs, as a result of which the equilibrium with only uninfected individuals disappears. It brings the system into the irrelevant, and hence ignored, region IV, in which (0,0) is the only remaining (and stable) equilibrium, which means that even an uninfected population cannot be maintained.

(b) *Phase plane analysis*

Let us fix the value of c, and pass through the different regions in figure 1*a* by varying the value of α. In figure 2 we plot the phase planes of F_i and F_u for the three different regions. In all three cases (0,0) is an attractor. Owing to the sexual reproduction, too small a population size always drives the population to extinction; this is the so-called Allee effect.

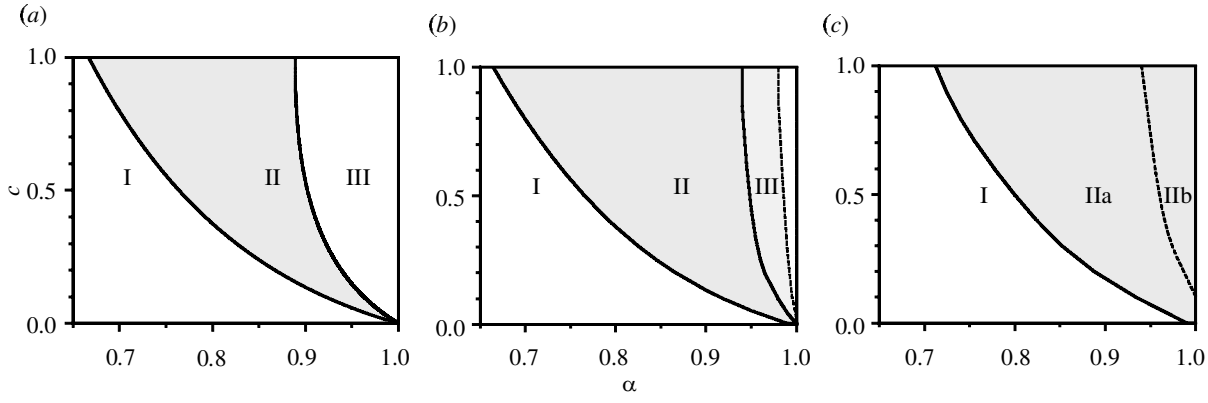

Figure 1. Bifurcation diagrams for the different models with the transmission efficiency (α) along the x-axis and the level of fitness compensation (c) along the y-axis: (*a*) the ODE model ($\delta = 0.04$); (*b*) the reshuffled CA model ($\delta = 0.4$); and (*c*) the spatial model ($\delta = 0.4$). In region I the male killer cannot invade; in region II there is stable coexistence of male killers and hosts; and in region III the entire population becomes extinct. The dashed line in (*b*) indicates the bifurcation line when the search space for mates is relatively large (eight automata), whereas for the solid line the search space is limited to two automata; the dashed line in (*c*) indicates the boundary between qualitatively different patterns.

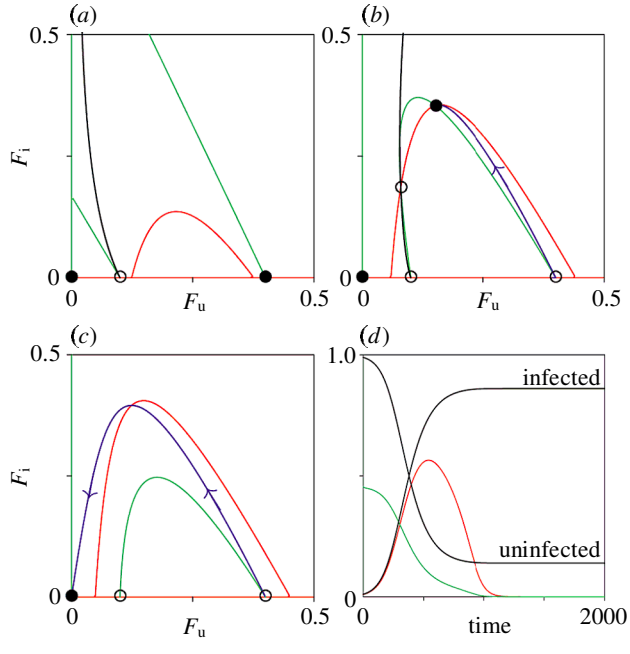

Figure 2. (*a*)–(*c*) Phase planes illustrating the three regions of qualitatively different behaviour in the ODE model; with uninfected females (F_u) along the x-axis and infected females (F_i) along the y-axis. Only α varies between the figures ($c = 1.0$ and $\delta = 0.04$) as follows: (*a*) region I: $\alpha = 0.60$; (*b*) region II: $\alpha = 0.87$; and (*c*) region III: $\alpha = 0.95$. The red lines denote the dF_i/dt nullclines and the green lines denote the dF_u/dt nullclines. In (*a*) and (*b*) the basins of attraction for the equilibria are shown in black. The white circles indicate unstable equilibria and the black circles indicate stable equilibria. The blue lines show trajectories starting with a small invasion of male killers ($F_i = 0.01$). (*d*) Time-plot (time in arbitrary units) in region III after a small initial infection ($F_i = 0.01$). The green line denotes the fraction of space occupied by uninfected hosts; the red line denotes the fraction occupied by infected hosts. The black lines represent infected and uninfected hosts by their fraction of the total population.

In region I (figure 2*a*) both invasion and maintenance of the male killer in the population are impossible. The only stable equilibrium besides (0,0) is the one with the hosts at their carrying capacity and no male killers. As a consequence, a male killer cannot spread when it is introduced into the system.

In region II (figure 2*b*) there is a stable equilibrium at which infected and uninfected individuals coexist. Figure 2*b* also shows the separatrix between the basins of attraction of the two stable equilibria, which is formed by the unstable manifold of one of the three saddle points. If the male killer is introduced into the system when the host population is close to its carrying capacity, the dynamics always lead to the stable equilibrium with both hosts and male killers in the population (the blue trajectory).

In region III (figure 2*c*) invasion of a male killer is also possible. However, when a male killer is introduced into the system, the number of infected individuals increases very rapidly, while the number of males declines. Owing to the shortage of males, the entire population eventually dies out.

(c) *High transmission efficiencies*

In previous models (Hurst 1991; Hurst *et al.* 1997; Freeland & McCabe 1997; Randerson *et al.* 2000) region III has not been observed, because, in contrast to our model, the number of males was never limiting and the total population size was always fixed, i.e. all fractions always added up to 1. In our model the population size is not fixed; instead, a variable fraction ($1 - F_i - F_u - M$) of the available space remains empty. Given the fixed population size, the criterion used by previous models for extinction of the population was that the fraction of infected females would become 1. Alternatively, if the fraction of infected/uninfected females (F_i/F_u) reached a stable value, they assumed that a non-trivial equilibrium had been reached. However, figure 2*d* shows that in region III in our model, where the population goes extinct, a stable fraction of F_i/F_u is also reached. The fraction is equal to the tangent of the angle at which the trajectory in phase space reaches (0,0). The equilibrium (0,0) is a

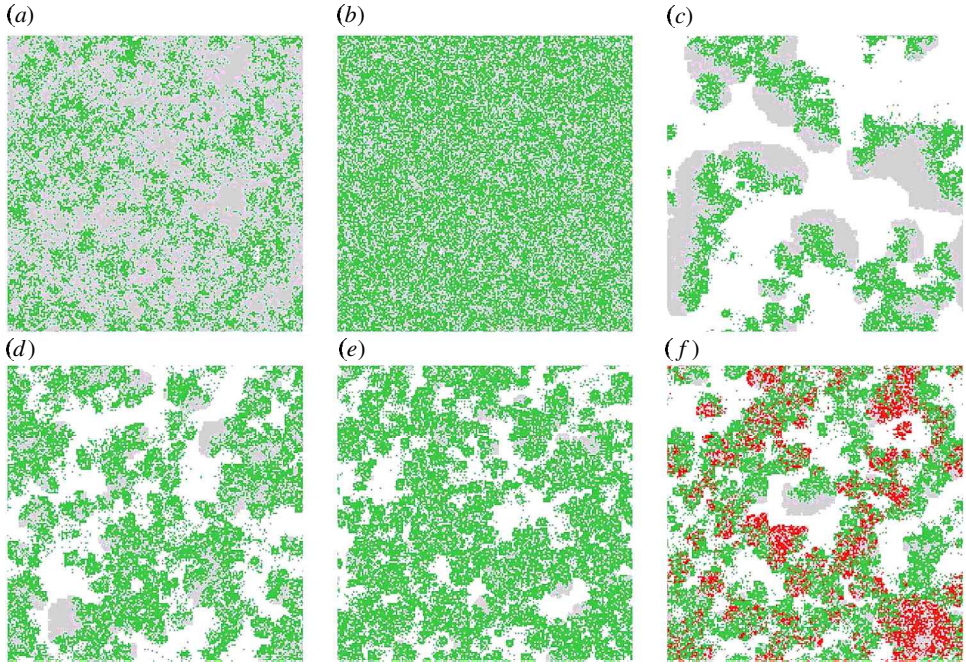

Figure 3. Snapshots of the CA showing different types of patterns. The infected individuals are green, the uninfected individuals are grey and the empty space is white; (*a*) and (*b*) show mixed patterns, (*c*) shows wave patterns, (*d*) and (*e*) show discordant waves and (*f*) shows two different coexisting male killers. The parameters are: (*a*) $\alpha = 1.0$, $c = 0.0$; (*b*) $\alpha = 0.90$, $c = 1.0$; (*c*) $\alpha = 1.0$, $c = 1.0$; (*d*) $\alpha = 1.0$, $c = 0.5$; (*e*) $\alpha = 0.97$, $c = 1.0$; and (*f*) red $\alpha = 0.90$, green $\alpha = 1.00$, $c = 1.0$ for both male killers.

stable star: both eigenvalues are the same ($\lambda_{1,2} = -\delta$). Consequently, close to the equilibrium the fraction of F_i/F_u does not change. Furthermore, if trajectories are started close to the carrying capacity of the uninfected individuals, all trajectories approach (0,0) at the same angle, because the trajectories will approach the unstable manifold of the equilibrium with the uninfected hosts at carrying capacity (see figure 2*c*). To conclude, a fraction of infected individuals in the population of less than unity does not guarantee survival of the population (see figure 2*d*).

This discussion also helps us to understand the effect that δ has on the location of the fold bifurcation line. If the death rate is higher, there is a larger fraction of empty space. If the fraction of empty space is large, the region in the phase plane that leads to extinction is also large, owing to difficulties in finding a male, which, in this system, is the limiting factor. Consequently, at higher values of δ the fold bifurcation moves towards lower values of α. In other words, when males are scarce, region III can be big; when males are not limiting, the region can be very small and moves towards the line $\alpha = 1$.

(d) *A perfectly transmitted male killer without fitness compensation*

Finally, there is the special case when $\alpha = 1$ and $c = 0$. In this case equations (2.3*a*) and (2.3*b*) are equal, i.e. there are no differences between the dynamics of the infected and the uninfected individuals. Therefore, the nullclines lie on top of each other, which leads to infinitely many equilibria. In this case the initial ratio of infected and uninfected individuals will remain constant: we do not call this invasion.

To summarize, in the ODE model, invasion of a male killer that is not fatal to the host population is only possible in region II. A perfectly transmitted male killer or a male killer with a sufficiently high transmission efficiency always drives the population to extinction (region III).

4. ANALYSIS OF THE RESHUFFLED CA

Next we look at the reshuffled CA, to determine to what extent the results in § 3 depend on the ODE model formalism that we have used. Figure 1*b* shows the bifurcation diagram for the reshuffled CA. It is very similar to that of the ODE, and the same three regions can be distinguished. The size of region III, however, does not depend strongly on the death rate: if the death rate is increased, the empty space is quickly filled. The size of region III, however, does depend on the availability of males. If the neighbourhood in which a female searches for mates is defined as the eight adjacent individuals, the region is small. If it is defined by four or two neighbours, region III becomes much larger (see figure 1*b*). Thus, changing the search space for males has an effect similar to changing the death rate in the ODE model.

5. ANALYSIS OF THE SPATIAL MODEL

In the spatial model there are only two regions of qualitatively different behaviour (see figure 1*c*). A male killer with a transmission efficiency of 1, or very close to 1, can spread in the spatial setting without driving the population to extinction. This is even the case without fitness compensation ($c = 0$). In other words, in the spatial model region III does not exist.

We will now discuss different combinations of c and α to look more closely at the differences between the spatial model and the mean-field models.

(a) *Perfect transmission without fitness compensation*

A perfectly transmitted male killer is able to spread even without fitness compensation. To understand this, we first have to note that production of females is more important than production of males, because one male can fertilize more than one female. Consequently, as long as there are enough males around, producing more females makes it possible to increase the number of individuals more rapidly. An empty automaton in an uninfected neighbourhood has maximally a 50% chance of becoming occupied by a female. An automaton in an infected neighbourhood, however, has a chance of up to 100% of becoming occupied by a female. Owing to the increasing shortage of males, more space in the infected neighbourhood remains empty and can be occupied by females during the next reproductive cycle, which is not true for space occupied by males. This is why infected individuals initially have an advantage. However, this only holds as long as there are sufficient males around. The male killer spoils his own local environment, by decreasing the number of males, until there are insufficient males available for the infected females to reproduce. This creates an indirect disadvantage for the infected individuals, compared with the uninfected individuals, which can spread into the empty space that is created by the male killer. Owing to these local and counteracting effects, a perfectly transmitted male killer can invade, but does not drive the population to extinction. Figure 3*a* shows a snapshot of the field after the initial transient period during which the male killer spreads through the population. The infection can spread, but small patches of empty space occur close to the infected areas.

(b) *Imperfect transmission without fitness compensation*

Even when the transmission efficiency is smaller than 1, there is still an increased probability of producing infected females, because, as described in § 5a, fewer males are produced, and more empty space is created that females can occupy. For lower values of α, the reproduction rate for the infected females simply becomes too low. The positive effect described can no longer compensate for the lower reproduction rate, and spread of the male killer becomes impossible. This behaviour corresponds to the behaviour in region I of figure 1*a*,*b*.

(c) *Perfect transmission with fitness compensation*

If we implement fitness compensation, a perfectly transmitted male killer still does not drive the population to extinction, even when the fitness compensation is 100% (see figure 1*c*). The infected females now spoil their own environment even more drastically, and the shortage of males causes large regions of local extinction. We observe wave patterns: the infection spreads very quickly and leaves an empty space behind. This empty space can only be filled by uninfected individuals, because they have males in their neighbourhood. If the fitness compensation is high, we observe large-scale wave patterns (see figure 3*c*); if the fitness compensation is low, we observe smaller scale and more discordant waves (see figure 3*d*).

(d) *Imperfect transmission with fitness compensation*

To obtain some understanding of the relative fitnesses of different male-killing strains, we first look at infection levels reached by the different strains. In general, it is assumed that the strain that is able to reach the highest level of infection should be able to outcompete the other strain(s).

For low values of c ($0 < c < 0.1$), the male killer with the highest transmission efficiency reaches the highest level in the population (see figure 4*c*). For higher values of c, however, there is an optimum at transmission efficiencies lower than 1 (see figure 4*a*). The dashed line in figure 1*c* indicates the 'ridge' with the highest levels of infection.

It turns out that this curve splits region II into two subregions with different spatial–temporal dynamics of infected and uninfected hosts. For high levels of transmission (region IIb) wave patterns occur, in which infected hosts replace uninfected hosts, but are followed by an empty space when the infected females run out of males. By contrast, in region IIa no waves occur, and infected and uninfected insects are well mixed owing to the large production of uninfected individuals by infected females. Between these distinct patterns we observe a transitional region with very discordant waves: uninfected individuals can break through wavefronts formed by infected hosts, creating new wave-like structures (see figure 3*d*,*e*). Nevertheless, the dashed line in figure 1*c* serves as a relevant bifurcation line between qualitatively different spatial–temporal patterns that determine the survival of competing strains of male killers, as discussed in § 6.

6. MULTIPLE MALE KILLERS

(a) *Mean-field models*

In the ODE model, the coexistence of two male-killer strains with different transmission efficiencies or different fitness compensations is impossible: the strain with the highest c or α will win, i.e. the one with the highest growth rate. This is a specific case of the generic mechanism known as competitive exclusion. The reshuffled CA has the same behaviour as the ODE. As a consequence, selection will always be towards high values of c and α, towards region III, where the whole population will go extinct.

(b) *Spatial model*

In figure 5 we plot the outcomes of competition experiments between two male killers with different transmission efficiencies. Three different regions of behaviour can be observed: the higher transmission efficiency wins (region A, red); coexistence of the two male killers (region B, black); and the lower transmission efficiency wins (region C, green).

The competitive behaviour in regions A and C corresponds to the conclusions drawn from figure 4: the male killer with the transmission efficiency closest to the optimal value will outcompete the other. In region A there are mixed patterns and the higher transmission will win simply because that male killer spreads faster. In region C there are wave

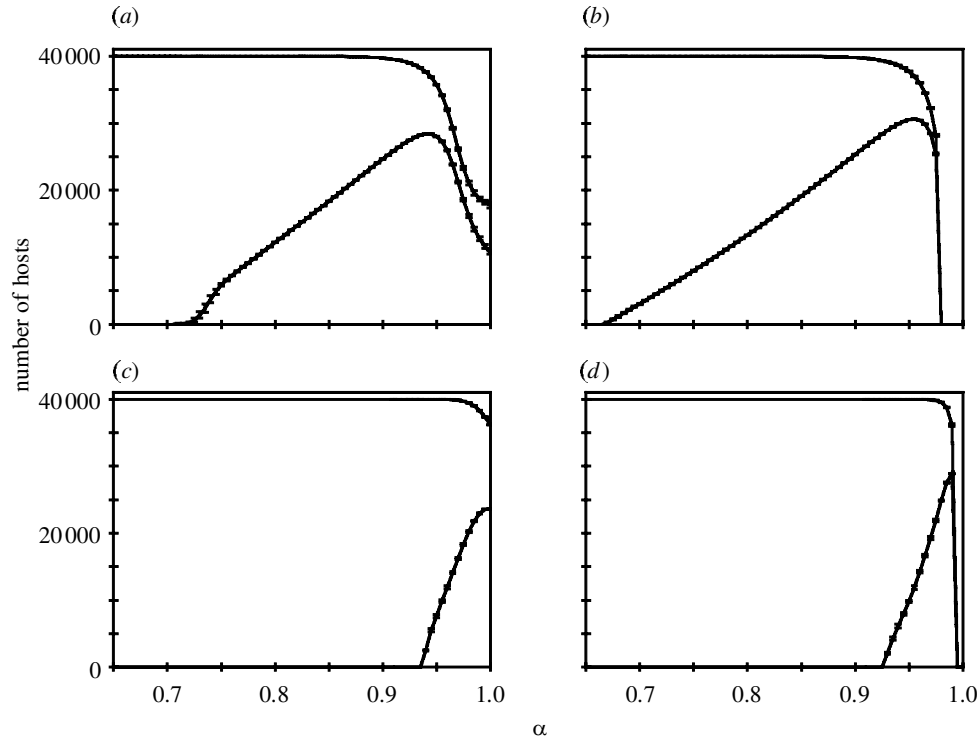

Figure 4. Levels of infection for different vertical transmission efficiencies (α) and fitness compensation values (c). (*a*) and (*c*) show the levels in the spatial model and (*b*) and (*d*) show the levels in the reshuffled CA. The lower lines show the number of infected hosts and the upper lines show the total number of individuals. The error bars indicate the very small standard deviations over 50 repeated runs: (*a*) and (*b*) $c = 1$; (*c*) and (*d*) $c = 0.1$.

patterns and the male killer with the lower transmission efficiency outcompetes the other because its infected females have better access to males, as described in § 5d.

Interestingly, in region B, coexistence of two male-killer strains is possible when they form different patterns, i.e. are from opposite sides of the bifurcation line in figure 1*c*. In other words, the occurrence of different patterns in the spatial model makes the coexistence of different male-killing strains possible. So, unlike the mean-field models, it is possible that a less-efficient male killer can coexist with a more-efficient male killer.

In figure 5*a* coexistence is measured after 1000 time-steps (500 years), while in figure 5*b* coexistence is measured after 4000 time-steps. Coexistence of two male killers with similar transmission efficiencies is, in the long run, unstable, but the coexistence of male killers producing different patterns is stable.

The patterns that can be observed in the CA during the competition experiments show all possible combinations of the patterns formed by the individual strains. In figure 3*f*, which shows the stable coexistence of two different strains, mixed regions created by the low-efficiency male killer can be observed together with regions of waves created by the high-efficiency male killer. Combinations can also be observed: there are wavelike structures where both the male killers are present.

7. DISCUSSION

Many studies have shown the existence of perfectly transmitted male killers in the field (Jiggins *et al.* 1998, 2000; Majerus *et al.* 1998, 2000). In classical non-spatial models (formulated as ODEs and difference equations), a perfectly transmitted male killer drives the population to extinction (Hurst 1991; Hurst *et al.* 1997; Freeland & McCabe 1997; Randerson *et al.* 2000). Owing to the incorporation of space, in our model it is possible for a perfectly transmitted male killer to both invade and be maintained in the population. The pattern formation prevents the perfectly transmitted male killer from driving the population to extinction.

Likewise, we have shown that explicitly incorporating space into the model is both a necessary and a sufficient condition to permit the invasion of male killers that do not confer a benefit in the form of fitness compensation, and for the permanent coexistence of two male killers with qualitatively different transmission efficiencies. Thus, in the spatial setting, such coexistence is possible without assuming the additional genetic mechanisms invoked by Randerson *et al.* (2000). We have shown that this difference between the spatial model and the non-spatial models is exclusively due to the implication of space and not caused by other, implicit, assumptions. We have proven this by comparing the reshuffled CA model with the ODE model: these two models behave very similarly.

It is interesting to note that over evolutionary time the non-spatial models would lead to the extinction of both hosts and male killers, because of positive selection for ever-larger transmission efficiencies. In the spatial model, evolution will not lead to extinction. Perfect transmission is a viable option. Moreover, evolution will not lead to perfect transmission, but to an 'optimal' transmission efficiency lower than 1, for which the male killers can obtain maximum density.

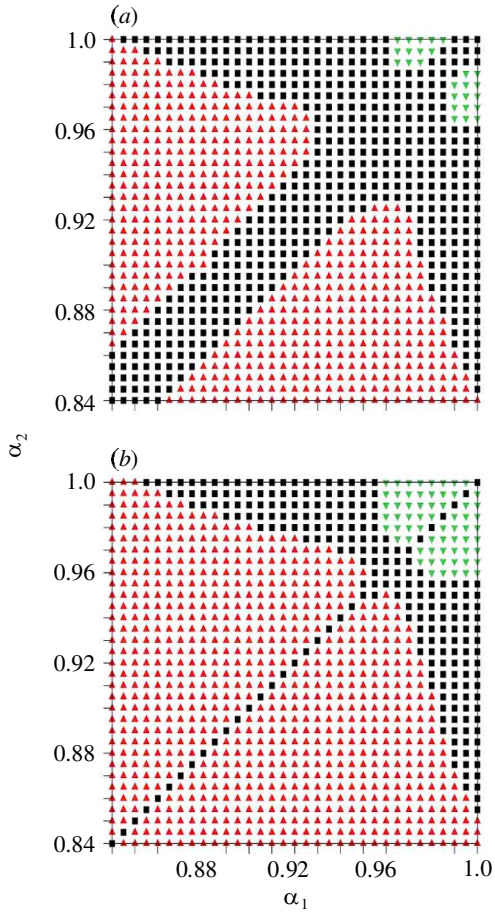

Figure 5. The outcomes of the competition experiments between male killers with different transmission efficiencies ($c = 1$). Along the axes are the transmission efficiencies of the male killers. In region A (red triangles) the male killer with the highest transmission efficiency wins, in region B (black squares) the two male killers coexist and in region C (green triangles) the male killer with the lowest transmission efficiency wins. The outcome of the competition is measured after (*a*) 1000 time-steps and (*b*) 4000 time-steps.

The persistence and coexistence of male killers that we observed in our model are caused by until now unobserved pattern formation. We believe that such patterns have not yet been observed because they are not easy to observe without targeted research. The patterns do not qualitatively change with the level of migration of the hosts. Counter-intuitively, more-dispersive hosts do not destroy the observed patterns, but merely enlarge the scale of the patterns (results not shown). In this paper we have taken only vertical transmission into account. In fact, the effects of horizontal transmission on the dynamics turned out to be negligible, and, so far, there has only been one example of horizontal transmission on the ecological timescale in the case of early male killing (Werren *et al.* 1986).

We still cannot explain quantitatively the coexistence found in *A. bipunctata* in Moscow (Majerus *et al.* 2000), where a very low transmission efficiency (81%) coexists with a very high one (up to 100%), as the invasion of the highly transmitted strain causes the extinction of a strain with a transmission efficiency lower than 85.5%. If hosts could have the opportunity in the CA to produce higher numbers of offspring (in our model maximally nine, see table 1), it might be possible to explain coexistence with much lower transmission efficiencies than the ones shown in figure 5. It is, of course, also possible that the low-efficiency male killer, a *Rickettsia*, has other fitness effects on the host than those of the other, highly transmitted, male killers (*Wolbachia* and a *Spiroplasma*).

What also remains unexplained is the coexistence of four male killers within the same population of *A. bipunctata* (Majerus *et al.* 2000). In simulations with higher numbers of male-killing strains, we found that, in all cases, at most two of them remain in the population. However, the transients before extinction are orders of magnitude longer than the competitive exclusion in the ODE with comparable differences in the transmission efficiency. If the efficiencies of the competing male killers are very close, the transient can be up to 55 000 time-steps (27 500 years), even in our relatively small 'universe'.

We expect that, as in our case, spatial-pattern formation can help to explain the existence of pathogens that cause parthenogenesis and feminization of males, as well as selfish genes, such as the mouse T complex (Van Boven & Weissing 1998).

In conclusion, this study adds one more specific case to the growing literature showing that the outcome of competition among replicators in space is qualitatively different from what we expect intuitively—or what is shown in mean-field models. Here, we show again how the fate of individuals depends on the dynamics of the spatial patterns that they create (Boerlijst & Hogeweg 1991; Savill *et al.* 1997; Pagie & Hogeweg 1999). We conclude that the time has come to require that investigations of ecological and evolutionary models should, by default, include the exploration of the consequences of spatial pattern formation.

The authors thank S. Marée for many fruitful discussions and his ever enthusiastic help with the manuscript. They also thank L. Keshet and two anonymous reviewers for helpful comments on the manuscript.

APPENDIX A: THE MODEL EQUATIONS

In the following, model equation (A 1) corresponds to equation (2.1), model equation (A 2) to equation (2.3*a*) and model equation (A 3) to equation (2.3*b*).

$$r = 1 + \frac{c\alpha}{2 - \alpha}, \tag{A 1}$$

$$\frac{\mathrm{d}F_\mathrm{i}}{\mathrm{d}t} = \frac{1}{2} r\alpha F_\mathrm{i} F_\mathrm{u}(1 - F_\mathrm{i} - 2F_\mathrm{u}) - \delta F_\mathrm{i}, \tag{A 2}$$

$$\frac{\mathrm{d}F_\mathrm{u}}{\mathrm{d}t} = \frac{1}{2} F_\mathrm{u}^2(1 - F_\mathrm{i} - 2F_\mathrm{u}) - \delta F_\mathrm{u} + \frac{1}{2} r(1 - \alpha) F_\mathrm{i} F_\mathrm{u}(1 - F_\mathrm{i} - 2F_\mathrm{u}). \tag{A 3}$$

APPENDIX B: DERIVATION OF TRANSCRITICAL BIFURCATION

For the transcritical bifurcation $\mathrm{d}F_\mathrm{u}/\mathrm{d}t = \mathrm{d}F_\mathrm{i}/\mathrm{d}t = F_\mathrm{i} = 0$, and $F_\mathrm{u} > 0$. Moreover, we must look only at non-trivial solutions (see figure 2).

$dF_i/dt = 0$:

$$\frac{1}{2}r\alpha F_u(1 - F_i - 2F_u) - \delta = 0\,, \tag{B 1}$$

$$F_i = 1 - 2F_u - \frac{2\delta}{r\alpha F_u}. \tag{B 2}$$

$F_i = 0$:

$$F_u = \frac{1}{4} \pm \sqrt{\frac{1}{16} - \frac{\delta}{r\alpha}}. \tag{B 3}$$

$dF_u/dt = 0$:

$$\frac{1}{2}F_u(1 - F_i - 2F_u) - \delta + \frac{1}{2}r(1 - \alpha)F_i(1 - F_i - 2F_u) = 0\,. \tag{B 4}$$

$F_i = 0$:

$$F_u = \frac{1}{4} \pm \sqrt{\frac{1}{16} - \delta}\,. \tag{B 5}$$

Combining equations (B 3) and (B 5) gives:

$$\frac{1}{4} \pm \sqrt{\frac{1}{16} - \frac{\delta}{r\alpha}} = \frac{1}{4} \pm \sqrt{\frac{1}{16} - \delta}\,, \tag{B 6}$$

$$r\alpha = 1 \tag{B 7}$$

and

$$c = 1 - \frac{3}{\alpha} + \frac{2}{\alpha^2}. \tag{B 8}$$

APPENDIX C: DERIVATION OF FOLD BIFURCATION

The fold bifurcation occurs if the dF_u/dt nullcline touches the dF_i/dt nullcline (see figure 2).

$dF_i/dt = 0$:

$$F_i = 1 - 2F_u - \frac{2\delta}{r\alpha F_u} \tag{C 1}$$

and

$$1 - F_i - 2F_u = \frac{2\delta}{r\alpha F_u}. \tag{C 2}$$

$dF_u/dt = 0$:

$$\frac{1}{2}F_u(1 - F_i - 2F_u) - \delta + \frac{1}{2}r(1 - \alpha)F_i(1 - F_i - 2F_u) = 0\,. \tag{C 3}$$

Substituting equations (C 1) and (C 2) into equation (C 3) gives:

$$\frac{1}{2}F_u\left(\frac{2\delta}{r\alpha F_u}\right) - \delta + \frac{1}{2}r(1 - \alpha)\left(1 - 2F_u - \frac{2\delta}{r\alpha F_u}\right)\left(\frac{2\delta}{r\alpha F_u}\right) = 0 \tag{C 4}$$

and

$$(\alpha(1 - 2r + r\alpha))F_u^2 + (r\alpha(1 - \alpha))F_u - 2\delta(1 - \alpha) = 0\,. \tag{C 5}$$

The nullclines touch each other when the discriminant equals zero, i.e.

$$r^2\alpha^2(1 - \alpha)^2 + 8\alpha(1 - 2r + r\alpha)\delta(1 - \alpha) = 0 \tag{C 6}$$

and

$$c = \frac{2\alpha^2 - 2\alpha - 8\alpha\delta + 16\delta - 4\sqrt{2\alpha^2\delta - 2\alpha\delta + 4\alpha^2\delta^2 - 16\alpha\delta^2 + 16\delta^2}(\alpha - 2)}{2\alpha(\alpha^2 - \alpha)}. \tag{C 7}$$

REFERENCES

Banks, C. J. 1955 An ecological study of Coccinellidae associated with *Aphis fabae* on *V. faba*. *Bull. Entomol. Res.* **46**, 561–587.

Boerlijst, M. C. & Hogeweg, P. 1991 Spiral wave structures in pre-biotic evolution: hypercycles stable against parasites. *Physica* D **48**, 17–28.

Freeland, S. J. & McCabe, B. K. 1997 Fitness compensation and the evolution of selfish cytoplasmic elements. *Heredity* **78**, 391–402.

Hoffmann, A. & Turelli, M. 1997 Cytoplasmic incompatibility in insects. In *Influential passengers: inherited microorganisms and arthropod reproduction* (ed. S. L. O'Neill, A. A. Hoffmann & J. H. Werren), pp. 42–80. Oxford University Press.

Hurst, L. D. 1991 The incidences and evolution of cytoplasmic male killers. *Proc. R. Soc. Lond.* B **244**, 91–99.

Hurst, G. D. D., Majerus, M. E. N. & Walker, L. E. 1992 Cytoplasmic male killing elements in *Adalia bipunctata* (Linnaeus) (Coleoptera: Coccinellidae). *Heredity* **69**, 84–91.

Hurst, G. D. D., Hurst, L. D. & Majerus, M. E. N. 1997 Cytoplasmic sex-ratio distorters. In *Influential passengers: inherited microorganisms and arthropod reproduction* (ed. S. L. O'Neill, A. A. Hoffmann & J. H. Werren), pp. 125–154. Oxford University Press.

Hurst, G. D. D., Graf von der Schulenburg, J. H., Majerus, T. M. O., Bertrand, D., Zakharov, I. A., Baungaard, J., Völkl, W., Stouthamer, R. & Majerus, M. E. N. 1999*a* Invasion of one insect species *Adalia bipunctata* by two different male-killing bacteria. *Insect Mol. Biol.* **8**, 133–139.

Hurst, G. D. D., Jiggins, F. M., Graf von der Schulenburg, J. H., Bertrand, D., West, S. A., Goriacheva, I. I., Zakharov, I. A., Werren, J. H., Stouthamer, R. & Majerus, M. E. N. 1999*b* Male-killing *Wolbachia* in two species of insect. *Proc. R. Soc. Lond.* B **266**, 735–740. (DOI 10.1098/rspb.1999.0698.)

Jiggins, F. M., Hurst, G. D. D. & Majerus, M. E. N. 1998 Sex ratio distortion in *Acraea encedon* (Lepidoptera: Nymphalidae) is caused by a male-killing bacterium. *Heredity* **81**, 87–91.

Jiggins, F. M., Hurst, G. D. D. & Majerus, M. E. N. 2000 Sex-ratio-distorting *Wolbachia* causes sex-role reversal in its butterfly host. *Proc. R. Soc. Lond.* B **267**, 69–73. (DOI 10.1098/rspb.2000.0968.)

Jiggins, F. M., Bentley, J. K., Majerus, M. E. N. & Hurst, G. D. D. 2001*a* How many species are infected with *Wolbachia*? Cryptic sex ratio distorters revealed to be common by intensive sampling. *Proc. R. Soc. Lond.* B **268**, 1123–1126. (DOI 10.1098/rspb.2001.1632.)

Jiggins, F. M., Hurst, G. D. D., Graf von der Schulenburg, J. H. & Majerus, M. E. N. 2001*b* Two male-killing *Wolbachia* strains coexist within a population of the butterfly *Acraea encedon*. *Heredity* **86**, 161–166.

Majerus, T. M. O., Majerus, M. E. N., Knowles, B., Wheeler, J., Bertrand, D., Kuznetzov, V. N., Ueno, H. & Hurst, G. D. D. 1998 Extreme variation in the prevalence of inherited male-killing microorganisms between three popu-

lations of Harmonia axyridis (Coleoptera: Coccinellidae). *Heredity* **81**, 683–691.

Majerus, M. E. N., Hinrich, J., Graf von der Schulenburg, J. H. & Zakharov, I. A. 2000 Multiple causes of male-killing in a single sample of the two-spot ladybird, *Adalia bipunctata* (Coleoptera: Coccinellidae) from Moscow. *Heredity* **84**, 605–609.

Pagie, L. & Hogeweg, P. 1999 Colicin diversity: a result of eco-evolutionary dynamics. *J. Theor. Biol.* **196**, 251–261.

Randerson, J. P., Smith, N. G. C. & Hurst, L. D. 2000 The evolutionary dynamics of male-killers and their hosts. *Heredity* **84**, 152–160.

Rousset, F., Bouchon, D., Pintureau, B., Juchault, P. & Solignac, M. 1992 *Wolbachia* endosymbionts responsible for various alterations of sexuality in arthropods. *Proc. R. Soc. Lond.* B **250**, 91–98.

Savill, N. J., Rohani, P. & Hogeweg, P. 1997 Self-reinforcing spatial patterns enslave evolution in a host-parasitoid system. *J. Theor. Biol.* **188**, 11–20.

Stouthamer, R., Breeuwert, J. A., Luck, R. F. & Werren, J. H. 1993 Molecular identification of microorganisms associated with parthenogenesis. *Nature* **361**, 66–68.

Toffoli, T. & Margolus, N. 1987 *Cellular automata machines*. Cambridge, MA: MIT Press.

Van Boven, M. & Weissing, F. J. 1998 Evolution of segregation distortion: potential for a high degree of polymorphism. *J. Theor. Biol.* **192**, 131–142.

Werren, J. H., Skinner, S. W. & Huger, A. M. 1986 Male-killing bacteria in a parasitic wasp. *Science* **231**, 990–992.

Werren, J. H., Hurst, G. D. D., Zhang, W., Breeuwer, J. A. J., Stouthamer, R. & Majerus, M. E. N. 1994 Rickettsial relative associated with male killing in the ladybird beetle (*Adalia bipunctata*). *J. Bacteriol.* **176**, 388–394.

As this paper exceeds the maximum length normally permitted, the authors have agreed to contribute to production costs.